ELSEVIER

Journal of Chromatography A, 781 (1997) 119–128

JOURNAL OF CHROMATOGRAPHY A

On-line concentration of neutral analytes for micellar electrokinetic chromatography
I. Normal stacking mode

Joselito P. Quirino*, Shigeru Terabe

Faculty of Science, Himeji Institute of Technology, Kamigori, Hyogo 678-12, Japan

Abstract

Using two anionic high-molecular-mass surfactants, butyl acrylate–butyl methacrylate–methacrylic acid copolymers, sodium salt (BBMA), and sodium 10-undecylenate (SUA) oligomer, and an anionic low-molecular-mass surfactant, sodium dodecyl sulfate (SDS), almost an order of magnitude improvement in concentration detection limit for a neutral analyte was made feasible by normal stacking mode (NSM). Stacking efficiency and recovery were independent of analyte retention factors and were slightly dependent on the nature of the pseudostationary phases. Furthermore, fundamental conditions for on-line sample concentration by NSM were theoretically and experimentally examined. © 1997 Elsevier Science B.V.

Keywords: Sample stacking; Sample handling; Micellar electrokinetic chromatography

1. Introduction

Micellar electrokinetic chromatography (MEKC), which was first introduced by Terabe et al. [1], is an electrokinetic separation technique for electrically neutral solutes that cannot be separated by capillary zone electrophoresis (CZE). Unlike CZE where the separation is primarily based on the difference in electrophoretic mobilities of the charged analytes, the separation mechanism in MEKC is based upon the partitioning of the neutral analytes between an electroosmotically pumped aqueous mobile phase and an electrophoretically retarded micellar phase. Although efficiencies can easily reach 100 000 theoretical plates for both CZE and MEKC, the major drawback is the low concentration sensitivity. Use of capillaries equipped with a bubble cell [2], sample preparation procedures with extraction or derivatization steps, and use of powerful detectors, such as laser-induced fluorescence detectors, are some approaches to solve this limitation. A simpler method is using on-line sample concentration; one method that has gained considerable attention is sample stacking [3–11]. Sample stacking works well with CZE, but simple transfer to MEKC seems to be exceptional since neutral analytes are unaffected by the enhanced field.

Liu et al. used sodium dodecyl sulfate (SDS) with a concentration slightly greater than the critical micelle concentration (CMC) in the sample matrix, and calculated a maximum sensitivity enhancement factor of 75 based on peak area counts with normal stacking mode (NSM) [10]. In this paper, we describe NSM in terms of improvement in concentration detection limit using peak heights, stacking efficiency, and recovery. Enhancement of the field in the sample zone was done by preparing the neutral analytes in water, thus stacking occurred with on-

*Corresponding author.

0021-9673/97/$17.00
PII S0021-9673(97)00498-6

column micellization. The effects of the nature of the surfactants, low-molecular-mass surfactant (LMMS) versus high-molecular-mass surfactant (HMMS), and analyte retention factors were also described.

2. Theory

2.1. General remarks

Preparing a neutral sample solution in a lower-conductivity matrix relative to the separation solution will enhance the field in the sample zone, providing micelles with electrophoretic velocities, $v_{ep}(mc)$, greater than those in the separation region. In the concentration boundary, micelles slow down and stack into very sharp concentrated zones. The migration velocity of a micelle v_{mc} is given as [12],

$$v_{mc} = v_{eof} + v_{ep}(mc) \quad (1)$$

where v_{eof} is the velocity of the electroosmotic flow. For a homogenous system,

$$v_{mc} = [\mu_{eof} + \mu_{ep}(mc)]E \quad (2)$$

where μ_{eof} is the mobility of the electroosmotic flow or the coefficient of electroosmotic flow, and $\mu_{ep}(mc)$ is the electrophoretic mobility of the micelle. The common separation solution used in MEKC is made of anionic micelles in a buffer at a pH greater than 6. Under these conditions and by considering the sign of each mobility and velocity as positive when movement is towards the cathode and negative when towards the anode, v_{mc} is positive according to Eq. (2), and movement of micelles is therefore directed towards the cathode where the detector is closely situated.

In sample stacking with hydrodynamic injection or NSM, a long plug of low-conductivity solution containing the sample (S) is injected into the capillary previously filled with a high conductivity separation solution or background solution (BGS) only. When voltage is applied, an enhanced field E_1 is experienced in the S region with higher resistivity R_1 (see Fig. 1A), the enhancement factor γ is given by Eq. (3) [5].

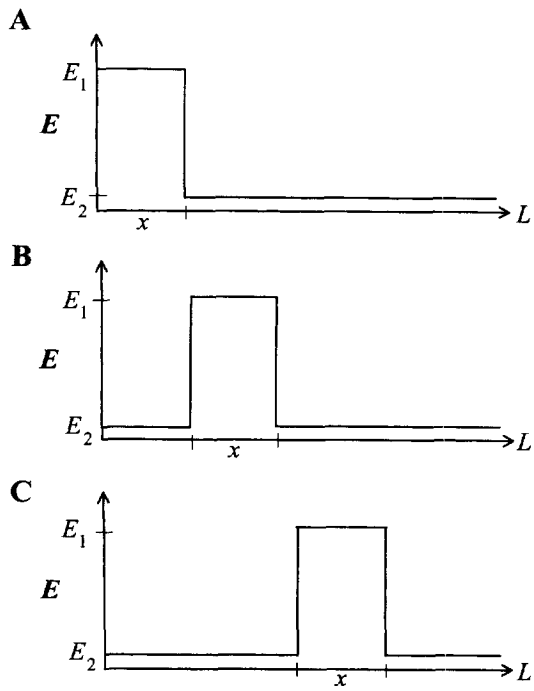

Fig. 1. Evolution of field strengths in S and BGS during stacking. (A) Starting situation; (B,C) after application of the electric field.

$$\gamma = \frac{R_1}{R_2} = \frac{E_1}{E_2} \quad (3)$$

E_2 and R_2 are field strength and resistivity in BGS region respectively. The field in the S and BGS regions was assumed to be constant throughout the electrophoresis if the entire S region stays inside the capillary (see Fig. 1).

The average electroosmotic flow velocity of the entire liquid inside the capillary $v_{eof}(ave)$ is proposed by Chien and Burgi [3] as,

$$v_{eof}(ave) = \frac{\gamma x v_{eof}(S) + (1-x)v_{eof}(BGS)}{\gamma x + (1-x)} \quad (4)$$

where $v_{eof}(S)$ and $v_{eof}(BGS)$ are the electroosmotic velocities when the whole capillary is filled with S or BGS alone. The value x between 0 and 1 is the fraction of the total length of capillary filled with S.

During stacking Eq. (1) can be rewritten as Eq. (5).

$$v_{mc} = v_{eof}(ave) + v_{ep}(mc) \quad (5)$$

The migration velocity of the micelles at the two regions would then be different since the field strengths are not the same; the migration velocity of micelles in the sample region $v_{mc}(S)$ and that in the separation region $v_{mc}(BGS)$ can then be derived assuming the same $\mu_{ep}(mc)$ in the two regions (Eq. (6a) and Eq. (6b)).

$$v_{mc}(S) = v_{eof}(ave) + v_{ep}(mc,S)$$

$$\text{where} \quad v_{ep}(mc,S) = \mu_{ep}(mc)E_1 \tag{6a}$$

$$v_{mc}(BGS) = v_{eof}(ave) + v_{ep}(mc,BGS)$$

$$\text{where} \quad v_{ep}(mc,BGS) = \mu_{ep}(mc)E_2 \tag{6b}$$

$v_{ep}(mc,S)$ and $v_{ep}(mc,BGS)$ are the electrophoretic velocities of the micelles in S and BGS, respectively.

2.2. Behavior of micelles in NSM

Assuming that micelles from BGS enter the plug of S prepared with water, the relative magnitude is proposed as follows:

$$|v_{ep}(mc,S)| > |v_{eof}(ave)| > |v_{ep}(mc,BGS)| \tag{7}$$

$v_{mc}(S)$ will then be negative and directed towards the anode according to Eq. (6a), while $v_{mc}(BGS)$ will then be positive and directed towards the cathode according to Eq. (6b). Using these magnitudes, the concentration of the micelle in the sample zone during stacking can be calculated. The connecting lines between Figs. 2A and 2B show the distances travelled by the boundary and micelles starting from the time voltage was applied (Fig. 2A). The concentration of the micelle in the sample zone $[mc]_S$ can simply be evaluated using Eq. (8), where $[mc]_{BGS}$ is the concentration of the micelle in BGS.

$$[mc]_S = \frac{v_{eof}(ave) - v_{mc}(BGS)}{v_{eof}(ave) - v_{mc}(S)} [mc]_{BGS} \tag{8}$$

This can be simplified to Eq. (9).

$$[mc]_S = \frac{v_{ep}(mc,BGS)}{v_{ep}(mc,S)} [mc]_{BGS} = \frac{[mc]_{BGS}}{\gamma} \tag{9}$$

Here we assumed that micelles entering the S zone do not contribute conductivity in the S zone.

A simple concentration profile of the micelles during stacking is described in Fig. 3. The concentration in the S plug of length x is zero initially (Fig. 3A) and rises to $[mc]_S$ from the front boundary (Fig. 3B) until x is filled with micelles (Fig. 3C). $[mc]_S$ remains constant throughout the process due to conservation of mass.

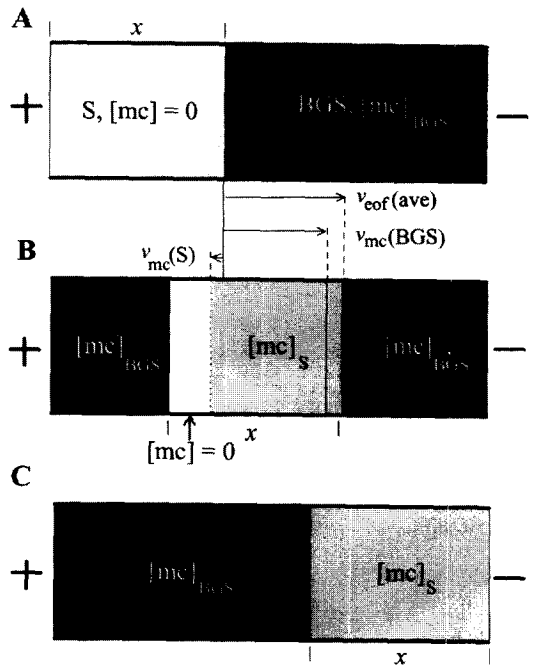

Fig. 2. Evolution of the migration of micelles and concentration boundary during stacking. (A) Starting situation; (B) after application of the electric field, the distance travelled by the concentration boundary, $v_{eof}(ave)$, the distance travelled by micelle from the concentration boundary in A, $v_{mc}(S)$, and the distance travelled by the micelle from the concentration boundary in A if the sample was dissolved in BGS, $v_{mc}(BGS)$; (C) situation when x is filled with micelle; plug length of S = x.

2.3. Behavior of neutral analytes in NSM

The effective electrophoretic velocity of a neutral analyte $v^*_{ep}(a)$ is given by Eq. (10).

$$v^*_{ep}(a) = \mu^*_{ep}(a)E \tag{10}$$

where E is the field strength and $\mu^*_{ep}(a)$ is the effective electrophoretic mobility of the neutral analyte a. The latter is given as Eq. (11) [13].

$$\mu^*_{ep}(a) = \mu_{ep}(mc)\frac{k}{1+k} \tag{11}$$

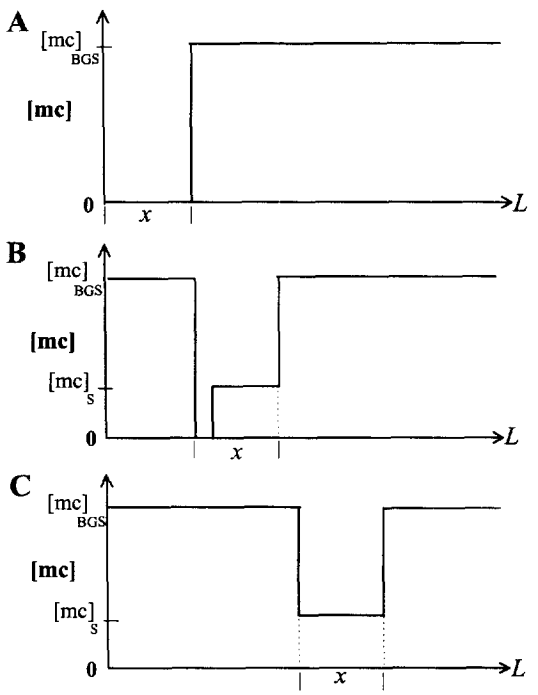

Fig. 3. Evolution of the concentration profiles of micelles emanating from BGS with time. (A) Starting situation; (B) appearance of micelles into a fraction of x, $[mc]_S$; (C) x filled with micelles, $[mc]_S$ persists until the plug is removed from the capillary.

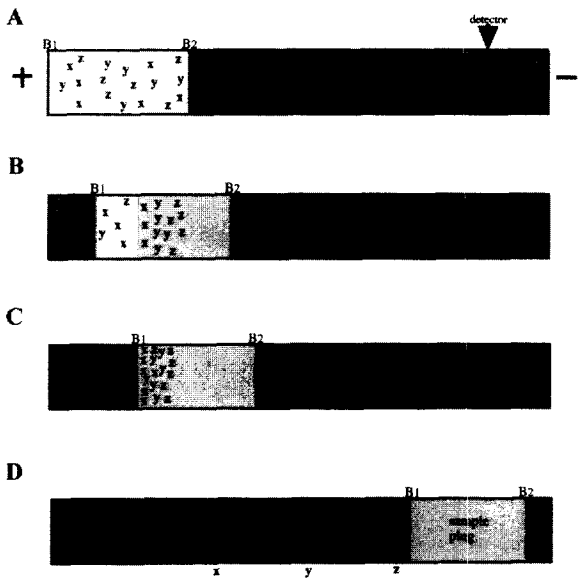

Fig. 4. Evolution of neutral analytes in S and BGS during stacking. (A) Starting situation; (B) high-velocity micelles in S carry the neutral analytes to the opposite concentration boundary B_1 in the order of decreasing retention factor $k(x)>k(y)>k(z)$; (C) neutral analytes stack in B_1 into thin concentrated zones; (D) analyte zones separate by virtue of MEKC.

where k is the retention factor of the neutral analyte.

Neutral solutes should have enough retention factors for them to be carried by the fast-moving micelles. The order of stacking of neutral analytes is dictated by their $v^*_{ep}(a)$ value in the S region. Generally, high-retention factor compounds are stacked first. In the sample region during the early stages of the stacking process, high-retention factor compounds travel faster (see Fig. 4B). The neutral analytes with high k will thus reach the opposite concentration boundary B_1 earliest (Fig. 4C), they eventually slow down to their corresponding $v^*_{ep}(a)$ in the BGS region and form a smaller volume of concentrated sample. The migration velocity of the S plug, v_S, can be assumed to be equal $v_{eof}(ave)$ since the entire liquid inside the capillary moves with one velocity. The boundaries B_1 and B_2 are not stationary but also then migrate with a velocity equal to v_S. v_S is much greater than the migration velocity of the stacked analytes, $v_a(BGS)$ ($v_S >>> v_a(BGS)$). The thin concentrated zone of neutral analyte formed will therefore leave the concentration boundary B_1 after sometime. The time when the thin concentrated zone of neutral analyte forms and leaves the stacking boundary B_1 depends on $v^*_{ep}(a)$ in the two regions. Finally separation of bands is shown in Fig. 4D.

3. Experimental

3.1. Apparatus

Capillary electrophoresis and stacking were carried out on a Beckman P/ACE 5000 capillary electrophoresis instrument (Fullerton, CA, USA) with Beckman Gold Software and a Hewlett-Packard 3D capillary electrophoresis system (Waldbronn, Germany), both equipped with fused-silica capillaries of 50 μm I.D. obtained from Polymicro Technologies (Phoenix, AZ, USA). Capillaries were thermostated at 20°C. Wavelengths of detection for each analyte were chosen using spectral absorbance curves recorded using a diode array detector. Conductivity of sample and separation solutions were

measured using a Horiba ES-12 conductivity meter (Kyoto, Japan).

The capillaries were washed daily, as a conditioning regimen, with 1 *M* NaOH (10 min), followed by methanol (5 min), 0.1 *M* NaOH (5 min), purified water (5 min), and finally with the electrophoresis buffer (5 min). The capillaries were flushed, between consecutive analyses to ensure repeatability, with 1 *M* NaOH (1 min), followed by methanol (1 min), 0.1 *M* NaOH (1 min), purified water (2 min), and finally with the electrophoresis buffer (2 min).

3.2. Samples and reagents

All solutions were prepared from water purified with a Milli-Q system (Millipore, Bedford, MA, USA) and were filtered through 0.45-μm filters (Toyo Roshi, Japan) prior to use. All chemicals were obtained in the finest grade available. Phenol, resorcinol, 2-naphthol, 1-naphthol, sodium tetraborate, phenanthrene, methanol, and SDS were purchased from Nacalai Tesque (Kyoto, Japan). Sodium dihydrogenphosphate and phosphoric acid were obtained from Wako (Osaka, Japan). Sample stock solutions were prepared with concentrations depending on their solubility in water. Stock solutions were diluted with water, diluted buffer, or diluted separation solution to give concentrations that yielded sufficient peak heights. Buffers were prepared accordingly from 100 m*M* sodium dihydrogenphosphate, 100 m*M* sodium tetraborate, and 0.3 *M* phosphoric acid stock solutions. Separation solutions were prepared by dissolving appropriate amounts of surfactant into the pertinent separation buffers. Butyl acrylate–butyl methacrylate–methacrylic acid copolymers, sodium salt (BBMA) supplied by Dai-ichi Kogyo Seiyaku (Kyoto, Japan) was purified by dialysis and freeze drying. Sodium 10-undecylenate (SUA) oligomer was synthesized by Mr. K. Iida in our laboratory following the procedures found in the literature [14]. Retention factors were determined using phenanthrene as the marker of the micelle and methanol as the marker of electroosmotic flow.

3.3. Procedure

Stacking was performed by injecting sample solutions for a much longer time compared to usual hydrodynamic injection. Sample solutions were introduced at the anodic end of the capillary at 50 mbar and voltage applied at positive polarity. Optimum plug length was assessed by injecting at different intervals and looking at the peak shapes. A length corresponding to the 40-s injection was chosen since it gave a good gaussian peak shape compared to longer injection times.

4. Results and discussions

4.1. Choice of sample matrix

Buffer and/or surfactant concentration in the S region did not significantly affect stacking. The initial presence of micelles in the sample zone is, therefore, not necessary to induce stacking. Fig. 5 shows that the peak height improvement of a 15-s

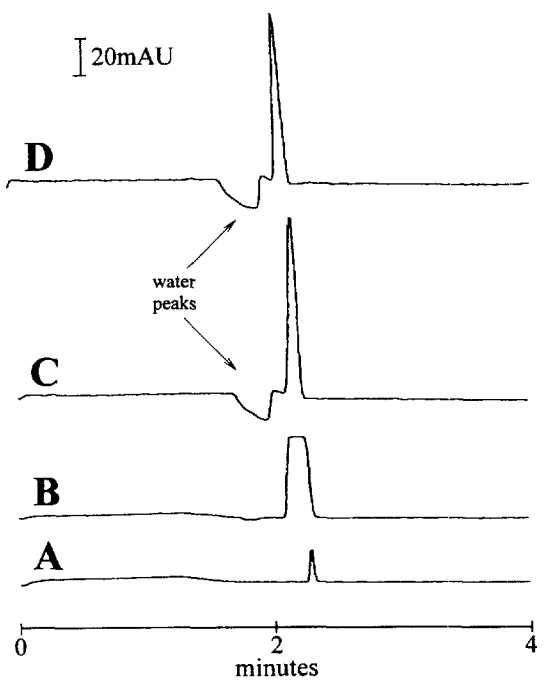

Fig. 5. Comparison of peak heights and shapes among different sample matrices. Sample matrix, BGS (A,B), 10 m*M* SDS in 7.5 m*M* sodium tetraborate (C), water (D); injection time, 2 s (A), 15 s (B–D); sample, resorcinol; BGS, 50 m*M* SDS in 37.5 m*M* sodium tetraborate–0.3 *M* phosphoric acid (pH 8); capillary, 33.5 cm (25 cm to the detector); detection, 206 nm; applied voltage, 15 kV.

injection versus a 2-s injection, using water and a solution containing SDS above the CMC (C and D), are relatively comparable. Similar results were obtained when the sample was prepared in a solution containing 3 m*M* SDS or diluted buffer (5 and 2 m*M* borate buffer). Use of water as sample matrix rather than a buffer or BGS dilution will also provide greater ease of performance.

The conductivity of S (resorcinol in water) at 20°C was measured to be 4.1 and 5.8 mS/cm for the BGS. Although the water was purified, dissolution of gas (e.g. CO_2) from the atmosphere and introduction of impurities from the sample or vial were responsible for the conductivity of S. Using water in general as the sample matrix will produce enhancement factors of more than hundreds according to Eq. (3). Very low E_2 will then be experienced and almost no electrophoresis will occur in the BGS. The great mismatch of the electroosmotic flow velocities of S with water and BGS will generate disturbance in the concentration boundaries, and will result in some mixing of these zones and thus lower γ. This was verified by injecting a 1-s plug of neutral sample before and after injecting a 15-s plug of BGS or water in separate experiments (see Fig. 6A and Fig. 6B). It should be mentioned that, although the water solution causes serious mixing at the boundary, the mixing did not significantly degrade the efficiency on NSM. Also, note that the stacked zones are formed in the concentration boundary, where mixing is of lower magnitude (see Fig. 6B).

4.2. Comparison of HMMS and LMMS

To date, several high-molecular-mass surfactants with a CMC of essentially zero were reported [14–19]. In the present study, two HMMS, BBMA and SUA oligomer, were employed as pseudostationary phases as well as SDS. Unlike previous studies which emphasized the micellar composition of the sample matrix to facilitate stacking [10,11], nonmicellar solutions were utilized. We assumed that $[mc]_S$ during stacking will be equal to or greater than the CMC in the case of LMMS. Table 1 lists detection limits obtained for resorcinol (concentration range, 1.135×10^{-4} to 1.135×10^{-5} *M*) with the psuedostationary phases studied. Least-squares analysis equations and r values were the following: $y=0.9170x+1.1310$ and $r=0.9999$ (2 s, SDS); $y=0.9376x+2.2851$ and $r=0.9998$ (SDS); $y=0.9014x+1.8838$ and $r=0.9991$ (SUA); $y=0.9085x+2.1854$ and $r=0.9861$ (BBMA). y is the logarithm of peak height (AU) and x is the logarithm of the molar concentration of resorcinol. Peak heights were used since the uncertainty in measuring peak heights at low concentrations of sample is less than with peak areas. Almost one-fold improvement in concentration detection limit compared to the 2-s injection were obtained either with HMMS or LMMS, although peak shapes were sharper with HMMS (see Fig. 7). This is because, in NSM, the amount of analytes injected into the capillary was the same whichever surfactant was used. Moreover, the concentration of SDS in the sample region may have reached a value greater than the CMC as assumed. Although a value lower than the CMC of SDS was computed based on Eq. (9), mixing of S and BGS zones could have led to the increase in concentration of SDS in the S region.

4.3. Stacking efficiency (SE) and recovery (%R)

Stacking efficiencies in terms of peak height (SE_{height}) for each test analyte were computed to evaluate quantitatively the degree of stacking. A stacking efficiency of 10 and 100 is comparable to one and two orders of magnitude improvement in concentration detection limit, respectively, or the detector response was increased to 10 and 100 times, respectively: simply calculated by dividing peak heights obtained when stacking was performed, H_{stack}, by peak heights under usual conditions (e.g. 2-s injection) H (Eq. (12)). These heights were obtained from the same sample solution.

$$SE_{height}=\frac{H_{stack}}{H} \tag{12}$$

Reproducibility of the electroosmotic flow in CE seems to be a major factor influencing variation in peak area counts. To account for this discrepancy in MEKC, corrected peak area counts A_{corr} were computed using Eq. (13).

$$A_{corr}=\frac{A}{t_r} \tag{13}$$

where A is the measured area and t_r is the migration

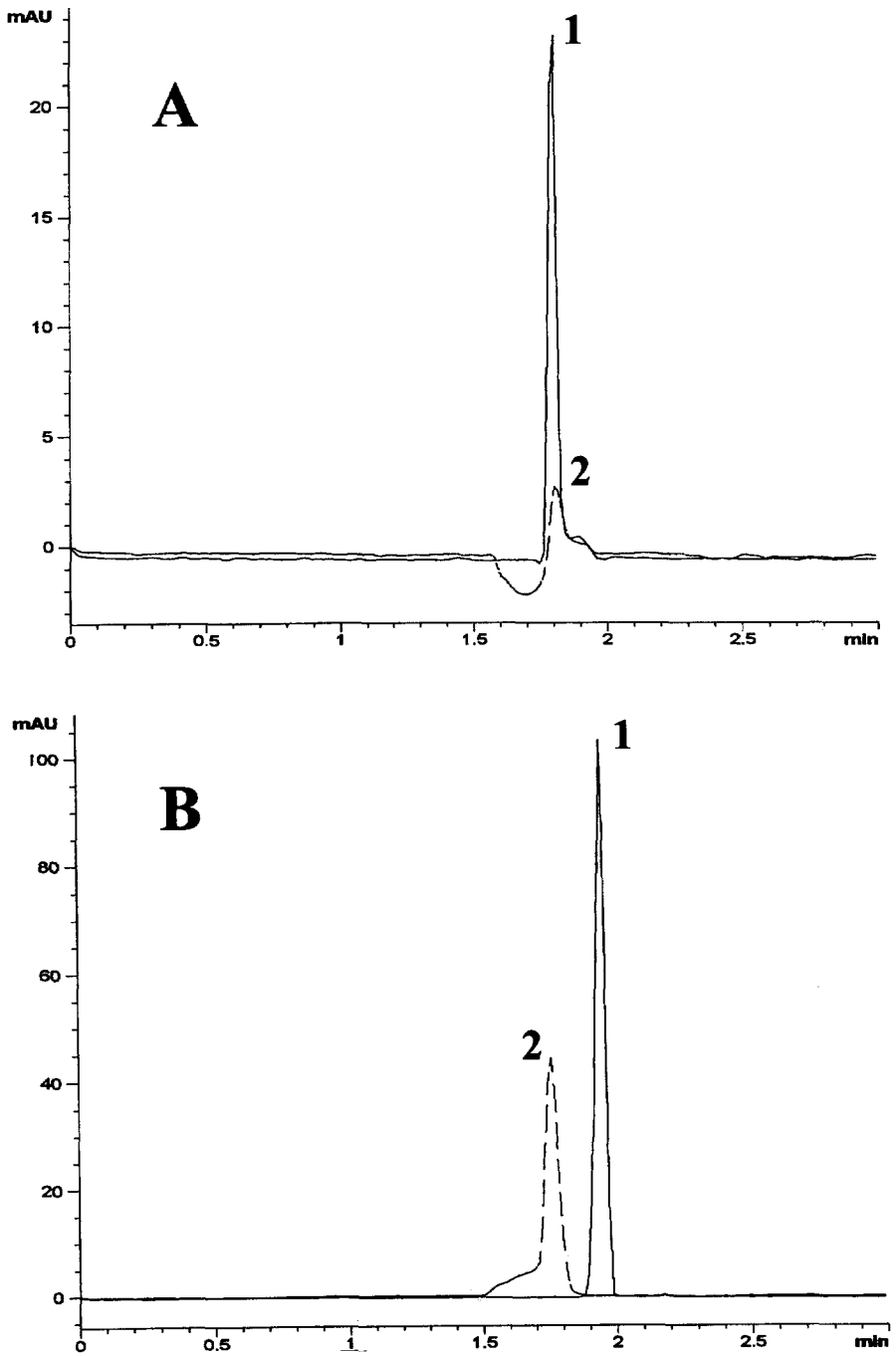

Fig. 6. Experimental verification of the mixing of S consisting of water and BGS during stacking. (A) Injection, 1 s of sample solution followed by 15 s of BGS (1) or water (2); (B) injection, 15 s of BGS (1) or water (2) followed by 1 s of sample solution; sample solution, phenol in water; BGS, 50 m*M* sodium tetraborate–0.3 *M* phosphoric acid (pH 8); S, plain water in this case; other conditions are the same as in Fig. 5.

Table 1
Effect of the nature of surfactants on stacking efficiency, recovery, and detection limit of resorcinol ($S/N=3$)

	100 m*M* SDS	1% SUA	1% BBMA
40-s injection NSM			
(a) SE_{height}	7	12	12
(b) *%R*	75	90	133
(c) detection limit	5.08×10^{-7} *M*	7.03×10^{-7} *M*	6.57×10^{-7} *M*
2-s injection			
detection limit	4.22×10^{-6} *M*		

All conditions are the same as in Fig. 7.

time of the neutral analyte. Stacking efficiency in terms of peak area SE_{area} were calculated using Eq. (14).

$$SE_{area} = \frac{A_{corr,stack}}{A_{corr}} \quad (14)$$

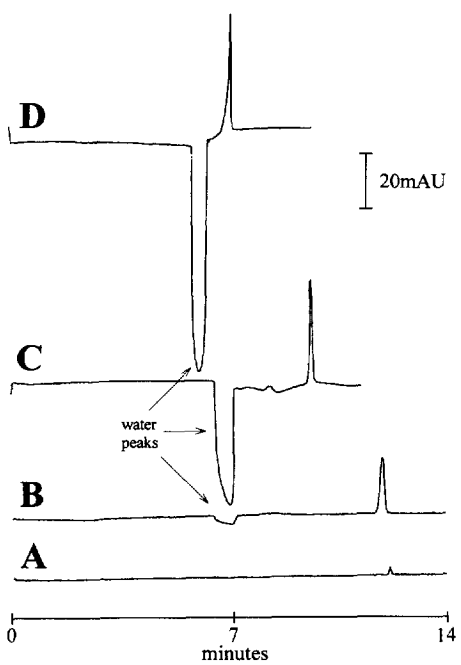

Fig. 7. Comparison of stacking effects among different surfactants. BGS, 100 m*M* SDS in run buffer (A,B), 1% SUA oligomer in run buffer (C), 1% BBMA in run buffer (D); injection time, 2 s (A), 40 s (B–D); S, resorcinol in water; run buffer, 50 m*M* sodium dihydrogenphosphate–100 m*M* sodium tetraborate (pH 8); capillary, 63.5 cm (55 cm to the detector); detection, 210 nm; applied voltage, 20 kV.

$A_{corr,stack}$ is the corrected area when stacking was performed and A_{corr} is the corrected area under usual conditions. SE_{area} is theoretically equal to the ratios of injected amounts of a sample. Percentages of each sample stacked based on peak areas or recoveries (*%R*) were assessed using Eq. (15).

$$\%R = \frac{SE_{area}\,(observed)}{SE_{area}\,(theoretical)} \times 100\% \quad (15)$$

The numerator is the stacking efficiency in terms of area computed based on Eq. (14) and the denominator is the stacking efficiency that is theoretically expected (e.g. for a 40-s injection NSM compared to a 2-s injection the value is 20). *%R* value is a measure of the amount of sample recovered from the water plug or the amount of sample stacked. A value of 100% will suggest that stacking was very efficient and no samples were lost.

Electropherograms (injection, 2 and 40 s) were generated from two different sample stock solutions with concentrations between 3×10^{-4} and 1×10^{-5} *M* for each test analyte. All experiments were carried out three times and the average values of SE_{height} and *%R* were calculated and are given in Tables 1 and 2.

Table 2
Effect of analyte retention factors on stacking efficiency and recovery with a BBMA solution

Analyte	*k*	SE_{height}	*%R*
Resorcinol	0.44	12	133
1-Naphthol	7.21	10	178
2-Naphthol	10.51	12	186

Detection, 210 nm (resorcinol), 226 nm (1-naphthol), 214 nm (2-naphthol). All other conditions are the same as in Fig. 7D.

4.4. Effect of the nature of pseudostationary phases and analyte retention factors on stacking efficiency and recovery

SE_{height} and $\%R$ for resorcinol obtained with a LMMS were merely more than half of those obtained with HMMSs (see Table 1). This was perhaps due to the stable molecular micelle structure of HMMS. A relatively low $\%R$ (75%) using SDS suggests that some fraction of the sample was not stacked as a peak, probably because the SDS micelle concentration was too low to cause efficient stacking. SE_{height} values were fairly in agreement with concentration detection limit data found in Table 1. Deviations can be attributed to the fact that concentration detection limits are dependent on signal-to-noise ratios.

Table 2 lists SE_{height} and $\%R$ for test analytes with different retention factors. All computed values of SE_{height} were comparatively close for all the test solutes. SE_{height} is therefore independent of retention factors and solely dependent on the amount of sample that can be injected into the capillary without distortion of peak shapes. All samples were 100% recovered and it is interesting to note that $\%R$ values were directly related to retention factors. More than 100% recovery is probably due to an unstable baseline caused by some impurity in BBMA.

In conclusion, this study improved the concentration sensitivity of MEKC for test analytes with reasonable solubility in water. We believe that NSM can be applied to solve detection problems related to the analysis of some real samples.

5. List of symbols

A_{corr}	corrected peak area counts
$A_{corr,stack}$	corrected peak area counts when stacking was performed
B_1	concentration boundary near the inlet vial
B_2	concentration boundary near the outlet vial
BGS	high conductivity separation solution or background solution
E	field strength
E_1	field strength in S zone
E_2	field strength in the BGS zone
γ	enhancement factor
H	peak height for a 2-s injection of the same sample solution used for H_{stack}
H_{stack}	peak height obtained when stacking was performed
k	retention factor
$[mc]_{BGS}$	concentration of the micelle in BGS
$[mc]_S$	concentration of the micelle in S zone during stacking
μ_{eof}	electroosmotic flow mobility or coefficient of electroosmotic flow
$\mu_{ep}(mc)$	electrophoretic mobility of micelle
$\mu^*_{ep}(a)$	effective electrophoretic mobility of neutral species a
R_1	resistivity in S zone
R_2	resistivity in BGS zone
$\%R$	recovery or the percent of sample stacked based on corrected peak areas
S	low conductivity sample solution
SE_{area}	stacking efficiency in terms of peak height, also SE_{area} (observed)
SE_{area}(theoretical)	theoretically computed stacking efficiency in terms of peak area
SE_{height}	stacking efficiency in terms of peak height
t_r	migration time of neutral analyte
v_a(BGS)	migration velocity of the stacked analytes in BGS
v_{eof}	electroosmotic flow velocity of a homogenous system
v_{eof}(ave)	average electroosmotic flow velocity of the entire liquid inside the capillary containing portions of S and BGS
v_{eof}(BGS)	electroosmotic flow velocity of BGS

$v_{eof}(S)$	electroosmotic flow velocity of S
$v^*_{ep}(a)$	effective electrophoretic velocity of neutral species a
$v_{ep}(mc)$	electrophoretic velocity of micelle
$v_{ep}(mc,BGS)$	electrophoretic velocity of the micelle in BGS
$v_{ep}(mc,S)$	electrophoretic velocity of the micelle in S
v_{mc}	migration velocity of micelle
$v_{mc}(BGS)$	migration velocity of the micelle in BGS zone
$v_{mc}(S)$	migration velocity of the micelle in S zone
v_S	migration velocity of S zone
x	fraction of the total length of capillary filled with S

Acknowledgments

The authors are thankful to Dr. K. Otsuka, Dr. N. Matsubara, and students of HIT for the support, and to Dr. P. Muijselaar for providing very valuable suggestions. JQ is also grateful to the Ministry of Education, Science, Culture, and Sports, Japan for the scholarship and the University of the Philippines Manila for allowing him to go on leave. This work was supported in part by a Grant-in-Aid for Scientific Research (No. 07554040) from the Ministry of Education, Science, Culture, and Sports, Japan.

References

[1] S. Terabe, K. Otsuka, K. Ichihara, A. Tsuchiya, T. Ando, Anal. Chem. 56 (1984) 111–113.
[2] D.N. Heiger, M. Herold, R. Grimm, Applications of Hewlett-Packard 3D Capillary Electrophoresis System, vol. 1, Hewlett-Packard, Waldbronn, 1992.
[3] R.L. Chien, D.S. Burgi, Anal. Chem. 64(8) (1992) 489A–496A.
[4] D.S. Burgi, R.L. Chien, J. Microcol. Sep. 3 (1991) 199–202.
[5] D.S. Burgi, R.L. Chien, Anal. Chem. 63 (1991) 2042–2047.
[6] R.L. Chien, D.S. Burgi, J. Chromatogr. 559 (1991) 141–152.
[7] R.L. Chien, D.S. Burgi, J. Chromatogr. 559 (1991) 153–161.
[8] R.L. Chien, J.C. Helmer, Anal. Chem. 63 (1991) 1354–1361.
[9] R.L. Chien, D.S. Burgi, Anal. Chem. 64 (1992) 1046–1050.
[10] Z. Liu, P. Sam, S.R. Sirimanne, P.C. McClure, J. Grainger, D.G. Patterson, J. Chromatogr. A 673 (1994) 125–132.
[11] K.R. Nielsen, J.P. Foley, J. Chromatogr. A 686 (1994) 283–291.
[12] J. Vindevogel, P. Sandra, Introduction to Micellar Electrokinetic Chromatography, Hüthig, Heidelberg, 1992.
[13] K. Gowsi, J.P. Foley, R.J. Gale, Anal. Chem. 62 (1990) 2714–2721.
[14] C.P. Palmer, M.Y. Khaledi, H.M. McNair, J. High Resolut. Chromatogr. 15 (1992) 756–762.
[15] H. Ozaki, S. Terabe, N. Ichihara, J. Chromatogr. A 680 (1994) 117–123.
[16] H. Ozaki, A. Ichihara, S. Terabe, J. Chromatogr. A. 709 (1995) 3–10.
[17] C.P. Palmer, S. Terabe, J. Microcol. Sep. 8(2) (1996) 115–121.
[18] S. Yang, J.G. Bumgarner, M.G. Khaledi, J. High Resolut. Chromatogr. 18 (1995) 443.
[19] J. Wang, I.W. Warner, Anal. Chem. 66 (1994) 3773.